A time domain approach for the optimal control of wave energy converter arrays

Mohamed A. Shabara, and Ossama Abdelkhalik

Abstract—**Wave energy converters typically use various control methods to extract energy from ocean waves. The objective of the control system is to optimize the energy extraction process, taking into account the dynamics of the system and the wave conditions. The task of deriving the optimal control laws of wave energy converter arrays for regular and irregular waves using the Pontryagin minimum principle was previously investigated in the literature. The result is a combination of the singular arc and bang-bang control laws. For irregular waves, some complexity arises due to the radiation state-space representation, which requires ignoring the hydrodynamic coupling terms related to the added mass and radiation-damping coefficients; this reduces the computational complexity of the control force but adversely affects the solution's accuracy. Also, the derived control laws are specific to a particular wave condition. Recently, the optimal control of a flexible buoy wave energy converter was derived using the convolution representation for the radiation force. In this work, the optimal control laws of flexible buoy wave energy converters are modified to simulate wave energy converter arrays; then, the results are compared to those obtained by dropping the hydrodynamic radiation coupling terms. Although using a convolution representation adds computational complexity to the optimal control problem, it generates an equation that is generic to any wave condition, can be used with any wave spectrum, and provides an expression for the switching condition.**

Index Terms—**Optimal Control - Singular Arcs - Wave Energy Converters - WEC Arrays**

I. Introduction

THE earliest known report of wave energy converters dates back to the late 18^{th} century. In 1799, a French physicist named Girard and his son built a device called the "Machine of Girard" to harness wave power [1]. The machine consisted of a series of floating rafts connected by hinges and gears. As the waves moved the rafts, the motion was transmitted to a pump, which was used to lift water from a lower level to a higher level. Although the Machine of Girard was not a commercial success, it was an early attempt to capture wave energy and convert it into useful work. Since then, numerous designs and concepts for wave energy converters have been proposed and developed [2]–[5]. It's worth noting that while the Machine of Girard is considered one of the earliest documented wave energy converters, there may have been earlier, undocumented attempts or ideas related to wave power harnessing that are not widely known.

This work was supported by the National Science Foundation (NSF), USA, under Grant 2023436.

Mohamed A. Shabara is a Graduate Research Assistant, (email: mshabara@iastate.edu)

Ossama Abdelkhalik is Professor (email: ossama@iastate.edu)

Both authors are in the Aerospace Engineering, Iowa State University, Ames, Iowa, 50010

Digital Object Identifier:
https://doi.org/10.36688/ewtec-2023-472

When a certain WEC is tested and considered for mass production and industrialization, it is usually applied in arrays to reduce maintenance and operational costs [6]. One of the earliest theoretical studies on WEC arrays was done in 1977 by Budal [7], where he presented a theory for maximizing power absorption by oscillating point absorber arrays in linear waves. It demonstrates that when the bodies are arranged in a linear row with a spacing of one wavelength or less of the incident wave, the power absorption per body can increase significantly, allowing the system to absorb 100% of the wave power incident on its entire length.

One of the earliest optimal control methods of WEC is the Complex Conjugate Control; this method utilizes the concept of the complex conjugate of the incident wave to optimize power absorption (to maximize absorbed energy). This is done by setting the control reactance X_{opt} to a value that cancels out the reactance of the mechanical system [8]. The PTO system's reactance affects its ability to extract energy from ocean waves and return power to the water. When the reactance is non-zero, the PTO can achieve bidirectional power behavior, which requires costlier components, leading to increased running and initial costs [9].

The complex conjugate control is considered a spectral method that provides a theoretical optimal resonance condition, resulting in unrealistic large amplitudes and unrealistically large two-way energy transfers between the buoy and PTO [10]. Moreover, this method does not allow for physical constraint handling as well as nonlinear control forces. The literature review in this section will focus on the *analytical time-domain optimal control methods* used to derive the optimal control laws of WECs that involve singular arc control laws.

The time domain equation of motion of a single degree of freedom (DoF) point absorber (PA) in regular waves is given by Cummins Equation [11]:

$$(m + m_{\infty})\ddot{x}(t) + c\dot{x}(t) + kx(t) = f_{\text{ext}}(t) + u(t) \qquad (1)$$

where $m \in \mathbb{R}_+$ is the buoy mass, $m_{\infty}, c, k \in \mathbb{R}_+$ are the hydrodynamic added mass, hydrodynamic radiation damping, and the hydrostatic stuffiness coefficients, x is a map, $\ddot{x}, \dot{x}, x \in \mathbb{R}$ are the center of gravity (C.G) acceleration, velocity and displacement, f_{ext} is the hydrodynamic excitation force and u is the control force.

Refs. [10], [12], [13] solved the optimal control problem in the time domain as a constrained problem (using the Pontryagin Minimum Principle); the control force took the form $u = -Bu_2(t)x_2^2(t) + u_1(t)G$, where $u_1(t) \in [-1, 1]$, $u_2(t) \in [0, 1]$, B is a constant damping coefficient, and G is a positive large constant. With this linear force representation, the derived Hamiltonian is linear in the control force u, and hence the optimal solution, in general, is expected to have singular arcs [9], [14].

Refs. [10], [13] proposed that the optimal control of multi-DoF point absorber has a pure bang-bang behavior (this can be extended to WEC arrays); the bang-bang control is a control strategy characterized by a discontinuous control signal where the control force is constrained to two fixed values, transitioning abruptly between them (known as an on-off controller). The derived control law in [10], [13] exhibits the absence of singular arcs, meaning there are no ambiguous control points in the solution. However, this property is attributed to the assumption of a specific form for the control force in the analysis, leading to a search domain limited to a subset of the overall solution domain [11]. Ref. [9], [11] derived the control that accounts for a search domain that is not limited to a subset of the overall solution domain, resulting in a bang-singular-bang behavior, a similar approach is done in the current work.

Ref. [11] used the Pontryagin Minimum Principle (PMP) approach to derive the optimal laws for a single DoF point absorber in both regular and irregular waves for the regular waves. The resulting singular control law for regular waves is expressed as

$$u_{\text{sa}} = f_{\text{ext}}(t) - cx_2(t) - kx_1(t) - \frac{m}{2c}\frac{\partial f_{\text{ext}}}{\partial t} \tag{2}$$

and the switching condition is

$$\sigma = x_2(t) - \frac{1}{2c} f_{\text{ext}}(t) \tag{3}$$

where σ is the switching surface, and the final optimal control law is

$$u = \begin{cases} u_{\text{sa}} & \text{if } \sigma = 0 \\ \gamma & \text{if } \sigma > 0 \\ -\gamma & \text{if } \sigma < 0 \end{cases} \tag{4}$$

where γ is the control force saturation limit. It is worth noting that if there is no saturation limit on the control force, the control law becomes $x_2(t) = \frac{1}{2c} f_{\text{ext}}(t)$, which is the same result obtained from the complex conjugate control.

For irregular waves, Ref. [11] used the radiation states representation for the radiation damping such that (1) is modified to be [15]:

$$(m + m_\infty)\ddot{x}(t) + \boldsymbol{C}_{\text{r}} x_{\text{r}}(t) + kx(t) = f_{\text{ext}} + u \tag{5}$$

$$\dot{x}_{\text{r}}(t) = \boldsymbol{A}_{\text{r}} x_{\text{r}}(t) + \boldsymbol{B}_{\text{r}} x_2(t) \tag{6}$$

where $x_{\text{r}} \in \mathbb{R}^{n_r \times 1}$ is the radiation states vector, $\boldsymbol{A}_{\text{r}} \in \mathbb{R}^{n_r \times n_r}$, $\boldsymbol{B}_{\text{r}} \in \mathbb{R}^{n_r \times 1}$, and $\boldsymbol{C}_{\text{r}} \in \mathbb{R}^{1 \times n_r}$ are constant radiation matrices, the process of calculating these matrices are detailed in many references including Ref. [16]. To solve the optimal control problem for irregular waves using (5) and (6), [11] used the Laplace transformation approach, cumbersome when applying the Laplace inverse, to mitigate this complexity, [11] used the representative wave frequency (ω_s) and the significant wave height to obtain the control law. For their specific device and wave conditions ($\omega_s = \frac{2}{3}\pi$), the control law is:

$$u(t) = 4688 \sin(\frac{2}{3}\pi t) + 897 \cos(\frac{2}{3}\pi t) \tag{7}$$

Although this method is simple to apply to any device, it has the disadvantage that the resulting equation is applicable for specific wave conditions. When the wave condition changes, new calculations are required to obtain new control laws. Additionally, calculating the Laplace inverse becomes a cumbersome task for devices with multiple DoF or WEC arrays. The hydrodynamic added mass and radiation coefficient matrices are dense, resulting in coupled equations of motion, and ignoring these coupling terms is required to obtain the control law analytically as demonstrated in Ref. [17]. Also, this method does not provide an analytical expression for the switching condition.

Like the complex conjugate control, the bang-singular-bang requires a bidirectional power flow, ref. [17]–[19] proposed an analytical method to apply a constraint on the maximum allowable reactive power available in the control system. The proposed method adds a constraint $u(t) \circ x_2(t) \leq -\epsilon$ where ϵ is the available reactive power and "$\circ$" is the Hadamard product; in the same work, the authors also proposed accounting for the saturation limit "γ" in the optimal control problem formulation as $|u(t)| \leq \gamma$.

These inequality constraints are then converted to an equality constraint using slackness variables α and β as follows:

$$-u(t)x_2(t) + \epsilon = \alpha \tag{8}$$

$$-u(t) + \alpha = \gamma \tag{9}$$

The slackness variable for each equality constraint is determined by evaluating the corresponding Lagrange multiplier. If the equality constraint is satisfied, the slackness variable will be zero. If the constraint is violated, the slackness variable will be positive. Note that this power constraint method will not be applied in the current work as it is beyond the scope of this paper's objective.

Ref. [20] used the control laws derived in [17] to identify the optimal heterogeneous WEC array while controlled optimally, heterogeneous here means that the buoys are not identical; where cylindrical buoys are used, and the optimizer finds the optimal radius and drought for each device in the array. Different optimal layouts were identified for 3, 5, 9, and 13 buoy arrays. The optimal control formulation described in this paper will be tested on the same optimal array layout for three devices used in [20] as described in section IV.

As mentioned earlier, ref. [17] ignored the hydrodynamic coupling terms to facilitate the Laplace inverse step in the derivation and to reduce the computational cost required by the GA optimizer to find the optimal layout. Ref. [9] mitigated this problem by using the convolution formulation for the hydrodynamic radiation forces, although the convolution computation is computationally expensive compared to the radiation state-space approximation described in (5) and (6), it provides more accurate results.

The dynamic modeling and optimal control of a point absorber with multiple degrees of freedom are similar to that of an array of point absorbers; the optimal control laws derived should coordinate between the degrees of freedom or the array members to maximize the total energy harvested by the system.

To highlight this similarity, ref. [15] derived the dynamic model for variable-shape buoy (VSB) WECs in regular and irregular waves. For irregular waves, the equation of motion is:

$$(\boldsymbol{M} + \boldsymbol{M}_\infty(t))\,\ddot{\mathbf{x}} + \boldsymbol{D}\dot{\mathbf{x}} + (\boldsymbol{K} + \boldsymbol{K}_\mathrm{h}(t))\mathbf{x} = \boldsymbol{Q}_\mathrm{ext}(t) + \boldsymbol{Q}_\mathrm{rad}(t) - \boldsymbol{Q}_\mathrm{pto}(t) \quad (10)$$

where $\mathbf{x} \in \mathbb{R}^{n_d \times 1}$, n_d is the number of generalized coordinates (or DoF). $\boldsymbol{M}$, $\boldsymbol{M}_\infty(t) \in \mathbb{R}^{n_d \times n_d}$ are the generalized mass, and the generalized hydrodynamic added mass matrices associated with the DoF, $\boldsymbol{D} \in \mathbb{R}^{n_d \times n_d}$ is the generalized damping matrix associated with the material properties, $\boldsymbol{K}, \boldsymbol{K}_\mathrm{h}(t) \in \mathbb{R}^{n_d \times n_d}$ are the generalized material stiffness and the generalized hydrostatic stiffness matrices, finally, $\boldsymbol{Q}_\mathrm{ext}, \boldsymbol{Q}_\mathrm{rad}, \boldsymbol{Q}_\mathrm{pto} \in \mathbb{R}^{n_d \times 1}$ are the generalized excitation, radiation damping, and control forces, respectively.

It is worth noting that (10) is linear time-variant (LTV) because the VSB WEC buoy changes its shape actively depending on the incident wave.

For fixed-shape buoy (FSB) WEC arrays, the system becomes linear time-invariant (LTI), and the generalized damping and stiffness matrices associated with the material properties vanish, thus (10) is reduced to:

$$(\boldsymbol{M} + \boldsymbol{M}_\infty)\,\ddot{\mathbf{x}} + \boldsymbol{K}_\mathrm{h}\mathbf{x} = \boldsymbol{Q}_\mathrm{ext}(t) + \boldsymbol{Q}_\mathrm{rad}(t) - \boldsymbol{Q}_\mathrm{pto} \quad (11)$$

where n_d, in this case, becomes the number of devices in the array. This is similar to the equation derived in [21].

The generalized hydrodynamic radiation force is expressed as

$$\boldsymbol{Q}_\mathrm{rad}(t, \mathbf{x}_2) = -\int_0^t (\boldsymbol{K}_\mathrm{r}(t-\tau)\mathbf{x}_2(\tau))\,d\tau \quad (12)$$

where $\boldsymbol{K}_\mathrm{r} \in \mathbb{R}^{n_d \times n_d}$ is the retardation function describing the hydrodynamic radiation memory effects such that:

$$\boldsymbol{K}_\mathrm{r}(t) = \frac{2}{\pi}\int_{\omega_\mathrm{min}}^{\omega_\mathrm{max}} \boldsymbol{D}_\mathrm{rad}(t, \omega)\cos(\omega t)\,d\omega \quad (13)$$

where $\boldsymbol{D}_\mathrm{rad} \in \mathbb{R}^{n_d \times n_d \times n_\omega}$ is the hydrodynamic radiation damping matrix for the WEC array, and n_ω is the number of wave frequencies superimposed to form the irregular wave.

The hydrodynamic excitation force is expressed as [15]:

$$\boldsymbol{Q}_{ext}(t) = \sum_{j=1}^{n_\omega} \Re\left(\boldsymbol{Ex}_j\ \eta_j\ e^{\hat{i}(\omega_j t + \phi_j)}\right) \quad (14)$$

where $\boldsymbol{Ex} \in \mathbb{C}^{n_d \times n_w}$ is the hydrodynamic excitation force coefficient obtained from the boundary element method solvers (ex.: NEMOH), η is the wave elevation, and ϕ is the random phase shift.

This paper represents the first work to derive the optimal control law for WECs arrays using the PMP approach using the convolution representation of the radiation forces; the rest of this paper is described as follows, section II gives an overview on the PMP approach and details the optimal control problem formulation of WEC arrays, then section III derives the optimal control laws WEC arrays. The derived control laws are then implemented in section IV on a linear row three devices WEC array, where the effect of accounting for the hydrodynamic coefficients coupling terms is highlighted, finally, section V serves as a conclusion, summarizing the main points discussed in this paper and outlining potential avenues for future research.

II. Problem Statment

Pontryagin minimum principle (PMP) is used to find the system's optimal control law. PMP screens the potential solutions at each time step and identifies the candidate that minimizes the Hamiltonian. The Hamiltonian is a mathematical expression that represents the total energy of a system, including both kinetic and potential energy.

There are cases where the PMP may be unable to provide sufficient information about the control law. This can happen when there are infinite possible control candidates, or the stationary condition is not an explicit function of the control force. The stationary condition refers to a state where the system is not changing over time. If the stationary condition is not an explicit function of the control force, it may not provide useful information about the control law, and additional necessary conditions are required.

The objective of the WEC array optimal control problem $\mathcal{J}$ is to maximize the total harvested energy by the WEC arrays over time $t \in [0, t_f]$ such that

$$\mathcal{J} = -\int_0^{t_f} \boldsymbol{Q}_\mathrm{pto}^T \mathbf{x}_2 \quad (15)$$

where $\boldsymbol{Q}_\mathrm{pto} = [u_1\ u_2\ \dots\ u_{n_d}]^T$ accounts for the PTO force on the devices C.G. ($u_i \in \mathbb{R}^1, \forall i = 1, \dots n_d$).

It is worth noting that the controller could maximize the total array harvested energy by turning and detuning the devices independently in the array depending on the incident waves and the interactions between the devices.

The optimal control problem for irregular waves is formulated based on (11) and (15) as:

$$\begin{aligned}
\min_{\mathbf{x}_2, \boldsymbol{Q}_{pto}} \quad & \mathcal{J} = -\int_{t_0}^{t_f} \boldsymbol{Q}_\mathrm{pto}^T \mathbf{x}_2 dt \\
\text{s.t.} \quad & \dot{\mathbf{x}}_1 = \mathbf{x}_2, t \in [t_0, t_f], \\
& \dot{\mathbf{x}}_2 = \tilde{\boldsymbol{M}}^{-1}\left(-\boldsymbol{K}_\mathrm{h}\mathbf{x}_1 + \boldsymbol{Q}_\mathrm{hydro}(\mathbf{x}_2, x_3) - \boldsymbol{Q}_\mathrm{pto}\right), \\
& \dot{x}_3 = 1, \mathbf{x}_{10} = \mathbf{x}_1(t_0), \mathbf{x}_{20} = \mathbf{x}_2(t_0)
\end{aligned}$$

where $\boldsymbol{Q}_{\text{hydro}}(\mathbf{x}_2, x_3) = \boldsymbol{Q}_{\text{ext}}(x_3) + \boldsymbol{Q}_{\text{rad}}(\mathbf{x}_2, x_3) \in \mathbb{R}^{n_d \times 1}$, and $\tilde{\boldsymbol{M}} = \boldsymbol{M} + \boldsymbol{M}_\infty$. Noting that the system described in (11) is non-autonomous, the optimal control formulation is formulated based on an autonomous system. Hence, the time t is considered as a state $x_3 \in \mathbb{R}$.

The control force saturation limit is [9]:

$$\boldsymbol{Q}_{\text{pto}} \in U \triangleq \{\boldsymbol{Q}_{\text{pto}} : \boldsymbol{Q}_{\text{pto}}^{\text{min}} \leq \boldsymbol{Q}_{\text{pto}} \leq \boldsymbol{Q}_{\text{pto}}^{\text{max}}\} \forall t \in [t_0, t_f] \tag{16}$$

where $\boldsymbol{Q}_{\text{pto}}^{\text{max}}$, and $\boldsymbol{Q}_{\text{pto}}^{\text{min}}$ are the maximum and minimum saturation limits of the PTO control forces.

III. Optimal Control

This section derives the optimal control laws for WEC arrays in irregular waves. The derivation procedure follows the same steps as in [9]. First, the Hamiltonian H is constructed, then the necessary conditions for optimally are derived, which includes the adjoint equations $\dot{\boldsymbol{\lambda}} = -\partial H/\partial \mathbf{x}$, where $\boldsymbol{\lambda}$ is the Lagrange multipliers' vector, and the stationary condition $H_u = -\partial H/\partial \boldsymbol{Q}_{pto}^T$ [13].

The Hamiltonian is constructed as

$$H(\mathbf{x}, \boldsymbol{\lambda}, \boldsymbol{Q}_{\text{pto}}) = -\boldsymbol{Q}_{\text{pto}}^T \mathbf{x}_2 + \boldsymbol{\lambda}_1^T \mathbf{x}_2 + \boldsymbol{\lambda}_2^T \tilde{\boldsymbol{M}}^{-1} \times \Big(-\boldsymbol{K}_{\text{h}} \mathbf{x}_1 + \boldsymbol{Q}_{\text{ext}} + \boldsymbol{Q}_{\text{rad}} - \boldsymbol{Q}_{\text{pto}}\Big) + \lambda_3 \tag{17}$$

The Hamiltonian constructed in (17) is linear in control force $\boldsymbol{Q}_{\text{pto}}$, and a singular arc control law will be obtained. The adjoint equations are:

$$\dot{\boldsymbol{\lambda}}_1 = \Big(\tilde{\boldsymbol{M}}^{-1} \boldsymbol{K}_{\text{h}}\Big)^T \boldsymbol{\lambda}_2 \tag{18}$$

$$\dot{\boldsymbol{\lambda}}_2 = \boldsymbol{Q}_{\text{pto}} - \boldsymbol{\lambda}_1 - \Big(\tilde{\boldsymbol{M}}^{-1} \frac{\partial \boldsymbol{Q}_{\text{rad}}^T}{\partial \mathbf{x}_2}\Big)^T \boldsymbol{\lambda}_2 \tag{19}$$

$$\dot{\lambda}_3 = -\bigg(\tilde{\boldsymbol{M}}^{-1} \Big(\frac{\partial}{\partial x_3} \Big(\boldsymbol{Q}_{\text{ext}} + \boldsymbol{Q}_{\text{rad}}\Big)\Big)\bigg)^T \boldsymbol{\lambda}_2 \tag{20}$$

Accordingly, the stationary condition is expressed as:

$$H_u = -\mathbf{x}_2 - \tilde{\boldsymbol{M}}^{-T} \boldsymbol{\lambda}_2 = \mathbf{0} \Longleftrightarrow \boldsymbol{\lambda}_2 = -\tilde{\boldsymbol{M}}^T \mathbf{x}_2 \tag{21}$$

The stationary condition is not a function of the PTO control force "$\boldsymbol{Q}_{\text{pto}}$" and the high order maximum principle (HMP) are summoned to derive the additional necessary conditions to get the control laws [13]. These additional necessary conditions are derived by differentiating (17) with respect to the time state (x_3) an even number of times until a control law is obtained in the form

$$\frac{d^{2k}}{dt^{2k}} H_u\Big(\mathbf{x}, \boldsymbol{Q}_{\text{pto}}, \boldsymbol{\lambda}\Big) = \boldsymbol{G}_0 + \boldsymbol{G}_1 \boldsymbol{Q}_{\text{pto}}(t) = \mathbf{0} \tag{22}$$

where $k \in \mathbb{Z}_+$ is the order of singularity, i.e., the control law takes the form

$$\boldsymbol{Q}_{\text{pto}} = -\boldsymbol{G}_0/\boldsymbol{G}_1 \tag{23}$$

where $\boldsymbol{G}_1 \neq \mathbf{0} \;\; \forall t \in [t_1, t_2]$.

The first additional necessary condition is obtained by differentiating (21) to get:

$$\dot{H}_u = -\dot{\mathbf{x}}_2 - \tilde{\boldsymbol{M}}^{-T} \dot{\boldsymbol{\lambda}}_2 = \mathbf{0} \Longleftrightarrow \dot{\boldsymbol{\lambda}}_2 = -\tilde{\boldsymbol{M}}^T \dot{\mathbf{x}}_2 \tag{24}$$

Substituting (18) into (24) then integrating yields:

$$\boldsymbol{\lambda}_1 = -{\boldsymbol{K}_{\text{h}}}^T \mathbf{x}_1 - \boldsymbol{C} \tag{25}$$

where $\boldsymbol{C} \in \mathbb{R}^{n_d \times 1}$ is an integration constant.

Substitute (25), the 2nd constraint, and (19) in (24) we get:

$$\dot{H}_u = \boldsymbol{C}_2 \boldsymbol{Q}_{\text{pto}} + \boldsymbol{C}_1 \mathbf{x}_1 - \tilde{\boldsymbol{M}}^{-1}(\boldsymbol{Q}_{\text{ext}} + \boldsymbol{Q}_{\text{rad}}) - \Big(\tilde{\boldsymbol{M}}^{-T} \frac{\partial \boldsymbol{Q}_{\text{rad}}}{\partial \mathbf{x}_2}\Big) \mathbf{x}_2 - \boldsymbol{C} = \mathbf{0} \tag{26}$$

Where $\bar{\boldsymbol{C}}_2 = (\tilde{\boldsymbol{M}}^{-1} - \tilde{\boldsymbol{M}}^{-T})$, and $\bar{\boldsymbol{C}}_1 = (\tilde{\boldsymbol{M}}^{-1} \boldsymbol{K}_{\text{h}} + (\boldsymbol{K}_{\text{h}} \tilde{\boldsymbol{M}}^{-1})^T)$, $\bar{\boldsymbol{C}}_2$ is skew-symmetric, i.e., it is a coupling matrix for the generalized control force elements; these coupling effects are ignored when solving the problem in the s-domain.

Differentiating (26) to get an additional necessary condition yields:

$$\ddot{H}_u = \boldsymbol{C}_2 \frac{\partial \boldsymbol{Q}_{\text{pto}}}{\partial x_3} - \tilde{\boldsymbol{M}}^{-T} \frac{\partial \boldsymbol{Q}_{\text{rad}}}{\partial \mathbf{x}_2} \dot{\mathbf{x}}_2 + \boldsymbol{C}_1 \mathbf{x}_2 - \tilde{\boldsymbol{M}}^{-1} \frac{\partial}{\partial x_3}\Big(\boldsymbol{Q}_{\text{ext}} + \boldsymbol{Q}_{\text{rad}}\Big) - \Big(\tilde{\boldsymbol{M}}^{-T} \frac{\partial \boldsymbol{Q}_{\text{rad}}}{\partial x_3 \partial \mathbf{x}_2}\Big) \mathbf{x}_2 = \mathbf{0} \tag{27}$$

Rearranging (27) yields:

$$\dot{\mathbf{x}}_2 = -\Big(\tilde{\boldsymbol{M}}^{-T} \frac{\partial \boldsymbol{Q}_{\text{rad}}}{\partial \mathbf{x}_2}\Big)^{-1} \Big[\tilde{\boldsymbol{M}}^{-1} \frac{\partial}{\partial x_3}\Big(\boldsymbol{Q}_{\text{ext}} + \boldsymbol{Q}_{\text{rad}}\Big) - \boldsymbol{C}_2 \frac{\partial \boldsymbol{Q}_{\text{pto}}}{\partial x_3} + \Big((\tilde{\boldsymbol{M}}^{-T} \frac{\partial^2 \boldsymbol{Q}_{\text{rad}}}{\partial \mathbf{x}_2 \partial x_3}) - \boldsymbol{C}_1\Big) \mathbf{x}_2\Big] \tag{28}$$

Substituting the 2nd constraint into (28) and rearranging yields the required singular arc control law:

$$\boldsymbol{Q}_{\text{pto}}^{\text{sa}} = \boldsymbol{Q}_{\text{ext}} + \boldsymbol{Q}_{\text{rad}} - \boldsymbol{K}_{\text{h}} \mathbf{x}_1 + \tilde{\boldsymbol{M}} \Big(\tilde{\boldsymbol{M}}^{-T} \frac{\partial \boldsymbol{Q}_{\text{rad}}}{\partial \mathbf{x}_2}\Big)^{-1} \Big[\tilde{\boldsymbol{M}}^{-1} \frac{\partial}{\partial x_3}\Big(\boldsymbol{Q}_{\text{ext}} + \boldsymbol{Q}_{\text{rad}}\Big) - \boldsymbol{C}_2 \frac{\partial \boldsymbol{Q}_{\text{pto}}}{\partial x_3} + \Big((\tilde{\boldsymbol{M}}^{-T} \frac{\partial^2 \boldsymbol{Q}_{\text{rad}}}{\partial \mathbf{x}_2 \partial x_3}) - \boldsymbol{C}_1\Big) \mathbf{x}_2\Big] \tag{29}$$

This equation can be compared to the singular arc generalized PTO force derived in [9]. From the necessary condition in (24) one can write:

$$\mathbf{x}_2 = \Big(\tilde{\boldsymbol{M}}^{-T} \frac{\partial \boldsymbol{Q}_{\text{rad}}}{\partial \mathbf{x}_2}\Big)^{-1} \Big(\boldsymbol{C}_1 \mathbf{x}_1 - \tilde{\boldsymbol{M}}^{-1}(\boldsymbol{Q}_{\text{ext}} + \boldsymbol{Q}_{\text{rad}}) + \boldsymbol{C}_2 \boldsymbol{Q}_{\text{pto}} - \boldsymbol{C}\Big) \tag{30}$$

By integrating (30) one can get:

$$\mathbf{x}_1 = \int_{t_0}^{t} \bigg(\Big(\tilde{\boldsymbol{M}}^{-T} \frac{\partial \boldsymbol{Q}_{\text{rad}}}{\partial \mathbf{x}_2}\Big)^{-1} \Big(\boldsymbol{C}_1 \mathbf{x}_1 + \boldsymbol{C}_2 \boldsymbol{Q}_{\text{pto}} - \tilde{\boldsymbol{M}}^{-1}\Big(\boldsymbol{Q}_{\text{ext}} + \boldsymbol{Q}_{\text{rad}}\Big) - \boldsymbol{C}\Big)\bigg) d\sigma + \mathbf{x}_1(t_0) \tag{31}$$

t_0 is arbitrary, one can show that the constant $\boldsymbol{C} = \mathbf{0}$ by setting $t = t_0$.

Noting that, from (12), and the differentiation under the integral sign rules, one can write:

$$\frac{\partial \boldsymbol{Q}_{\text{rad}}}{\partial x_3} = -\boldsymbol{K}_{\text{r}}(0)\mathbf{x}_2(t) - \int_0^t \left(\dot{\boldsymbol{K}}_{\text{r}}(t-\tau)\mathbf{x}_2(\tau)\right) d\tau \tag{32}$$

$$\frac{\partial \boldsymbol{Q}_{\text{rad}}}{\partial \mathbf{x}_2} = -\int_0^t \left({\boldsymbol{K}_{\text{r}}}^T(t-\tau)\right) d\tau \tag{33}$$

$$\frac{\partial^2 \boldsymbol{Q}_{\text{rad}}}{\partial x_3 \partial \mathbf{x}_2} = -\boldsymbol{K}^T(0) - \int_0^t \left({\dot{\boldsymbol{K}}_{\text{r}}}^T(t-\tau)\right) d\tau \tag{34}$$

The derivation done in this section is proof of the following proposition:

Proposition 1. *For a WEC array, the control law that maintains*

$$H_u(\mathbf{x}, \boldsymbol{\lambda}) = 0, \quad \forall t \in [t_1, t_2] \subseteq [t_0, t_f] \tag{35}$$

for the optimal control problem defined in section II, if the PTO saturation limit is large enough, the problem becomes a singular arc optimal control problem. Thus, the optimal control law consists of both subarcs of singular control and non-singular (bang) control, and it is determined by the sign of the switching curves defined by the components of "$\boldsymbol{C}$"; the junctions between the control laws are discontinuous. We say a singular arc occurs if any of the switching functions $\dot{H}_{u_i} \forall i = 1, ..., n_d$ vanishes; $\dot{H}_{u_i}$ is defined as the switching surface that corresponds to Q_i^{pto}, and it is obtained from the necessary condition $\dot{H}_{u_i}$. The optimal control law that satisfies the two additional necessary conditions $\dot{H}_u$, $\ddot{H}_u$ and Legendre-Clebsch Condition $:= (-1)^k \frac{d}{du}\left(\frac{d^{2k}}{dx_3^{2k}}\right) H_u \geq 0 \; \forall t \in [t_1 \;\; t_2]$ is expressed as $\boldsymbol{Q}^{pto} = \begin{cases} \boldsymbol{Q}_{pto}^{sa} & \text{if } \boldsymbol{C} = \mathbf{0} \\ \boldsymbol{Q}_{pto}^{max} & \text{if } \boldsymbol{C} > \mathbf{0} \\ \boldsymbol{Q}_{pto}^{min} & \text{if } \boldsymbol{C} < \mathbf{0} \end{cases}$.

The optimal PTO force $\boldsymbol{Q}_{pto}$ components switch between the boundaries at the zero crossings of the corresponding function.

This proposition can be compared to the definition in [9].

IV. Results and Discussion

This paper derives the optimal control law of WEC arrays; the derivation in this paper is an extension to work done in [9], which addresses the optimal control law of single WECs with multiple degrees of freedom (specifically, the variable-shape wave energy converters). Ref. [20] used a genetic algorithm (GA) to find the optimal device dimensions in cylindrical WEC homogeneous arrays, and its results for three cylindrical devices are utilized in the paper. The WEC array layout and device dimensions used in this paper are listed in Table IV and Fig.1.

Also, the control force limit were set to be $\boldsymbol{Q}_{\text{pto}}^{\text{max}} = -\boldsymbol{Q}_{\text{pto}}^{\text{min}} = [10^5 \;\; 10^5 \;\; 10^5]^T$.

The Bretschneider wave spectrum is used in this paper [15] with a total number of waves of $n_\omega = 256$. The wave conditions used are listed in Table IV, also, fig. 2 shows the $\boldsymbol{Q}_{hydro}$ which is the summation of the excitation and radiation damping forces acting on the three devices.

TABLE I
THE HOMOGENEOUS ARRAY LAYOUT, DIMENSIONS, AND WAVE CONDITIONS

Symbol	Quantity	Unit
n_d	Number of devices	3
r	Radius	7.22 m
d	Drought	5.81 m
	Device 1 position	(0,0,0) m
	Device 2 position	(0,40.2554,0) m
	Device 3 position	(0,-40.2554,0) m
H_s	Significant wave height	0.8222 m
T_p	Particular wave period	6.00 sec
n_ω	Number of frequencies	256 sec
ω_{min}	Minimum frequency	0.1 rad/sec
ω_{max}	Maximum frequency	3.5 rad/sec

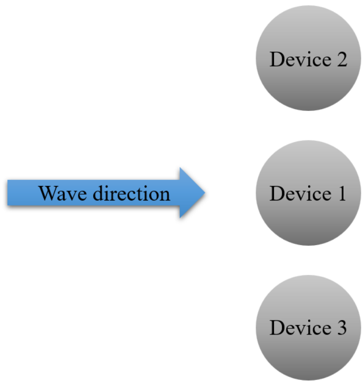

Fig. 1. Optimized size for an array of 3 devices

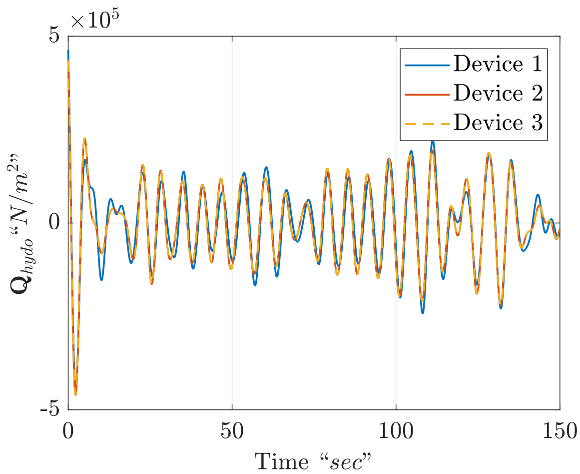

Fig. 2. The external hydrodynamic force $\boldsymbol{Q}_{hydro} = \boldsymbol{Q}_{ext} + \boldsymbol{Q}_{rad}$

To highlight the significance of the contribution of this work, two cases were tested; the first accounts for the radiation coupling terms (for the added mass and the radiation damping coefficients), and the second drops these coupling terms. Since the three devices are facing the incident in a parallel sense (Fig. 1), for both cases, buoys two and three should harvest the same energy due to the array layout symmetry about device 1.

Figures 3 and 4 show the heave displacements and velocities of the three devices; it can be seen that the re-

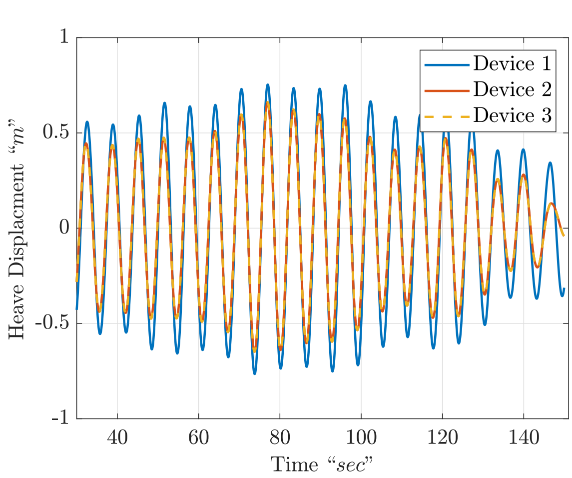

Fig. 3. Heave displacement response

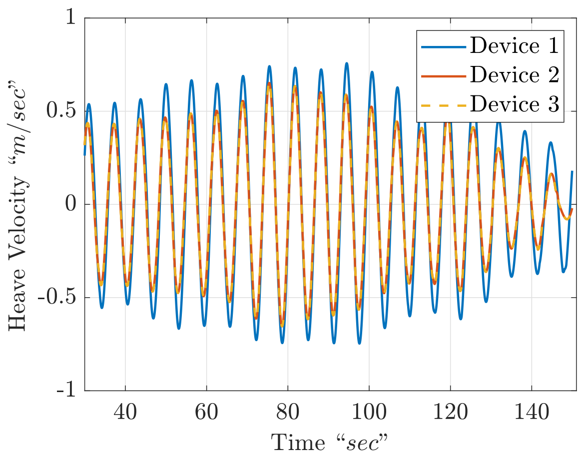

Fig. 4. Heave velocity response

sponse of devices 2 and 3 are identical due to the array layout symmetry about device 1, and device one's pk-pk displacement is higher than the other two devices; this suggests that the controller takes advantage of the radiated waves from both devices 3 and 2 to increase the harvested energy from device 1. It can be seen that due to the $\boldsymbol{Q}_{\text{PTO}}$ saturation limit, the displacement of device one is bounded by ± 0.76 m.

The control force $\boldsymbol{Q}_{\text{PTO}}$ for the three devices are shown in Fig. 5, the effect of the saturation limit ($10^5 N$) can be seen in the waveform, which causes a square waveform to be obtained. It is worth noting that the results show that the solution is a bang-singular-bang law. The more the saturation limit is relaxed, the more time the control spends in the singular phase.

The energy harvested by the three devices while accounting for the coupling terms of the hydrodynamic radiation forces is shown in Fig. 6; on the other hand, Fig. 7 shows the harvested without accounting for the coupling terms. In both cases, the device in the middle (device 1) harvests more energy most of the simulation time; also, it can be seen that ignoring the coupling terms results in a similar behavior of all three devices in the array, which device one harvesting slightly more energy compared to the other two devices.

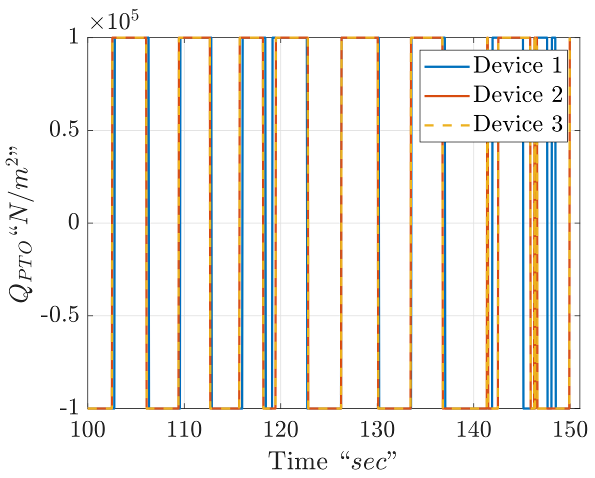

Fig. 5. PTO Control force $\boldsymbol{Q}_{\text{PTO}}$ showing the bang-singular-bang control law performance.

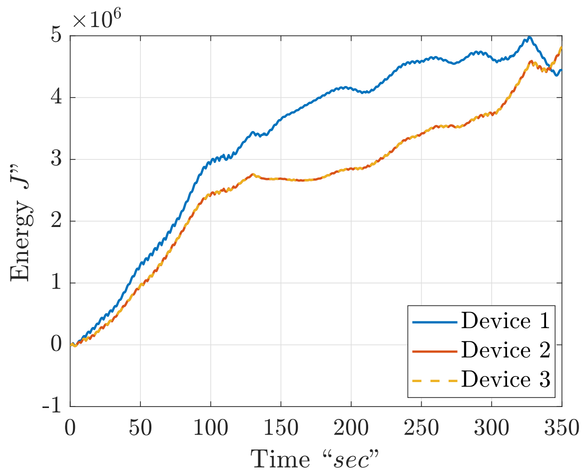

Fig. 6. Energy harvested while accounting for the coupling terms

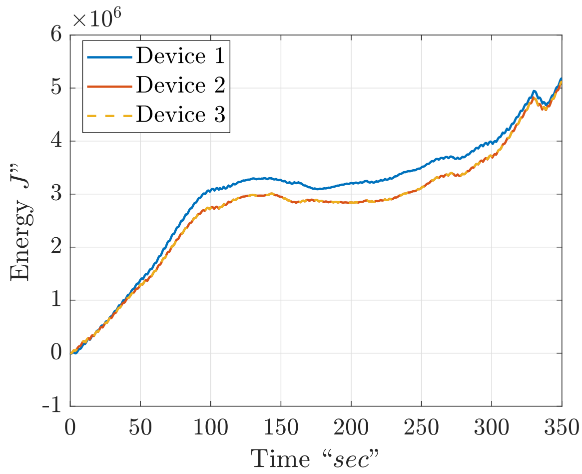

Fig. 7. Energy harvested: No coupling terms

Fig. 8 shows that ignoring the coupling terms leads to an overestimation in the harvested energy in the first 155 seconds; then, from 155 seconds to 340 seconds, it started underestimating the total energy harvested, then the opposite behavior happened from 340 seconds until the end of the simulation. Noting that the phase shift in the excitation force Eq. (14) is random, and

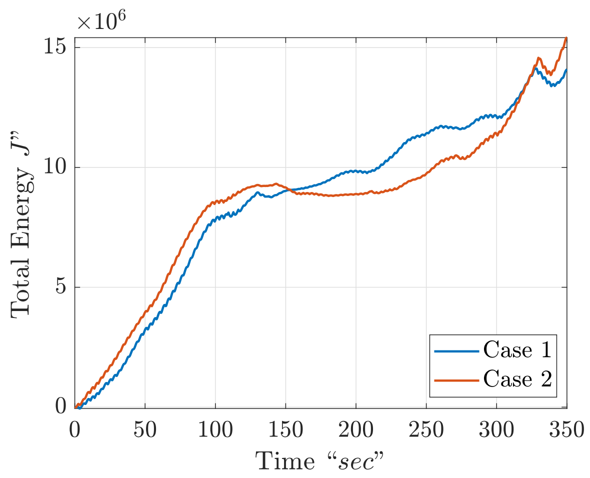

Fig. 8. Total energy harvested by the array:
Case 1: With the hydrodynamic radiation coupling terms.
Case 2: Without the hydrodynamic radiation coupling terms

different behavior can be obtained if different phase shift values are used.

The tested array in the current work consists of only three identical WECs, which are relatively large distances apart; it is expected that when increasing the number of WECs in the array and/or decreasing the distances between the devices, the overestimation/underestimation behavior would increase; i.e., in a layout optimization task, the radiation coupling terms can be pivotal.

V. Conclusion and Future Work

The optimal control laws for wave energy converter arrays were derived using Pontryagin's minimum principle; unlike the optimal control laws developed in the literature, this work accounts for the coupling terms associated with the radiation forces coefficients. The similarity between the optimal control derivation for WEC arrays and WECs with multiple degrees of freedom is highlighted in this work. Results show that, depending on the simulation time, ignoring the radiation coupling terms in an optimal WEC array arrangement overestimates/underestimates the generated power; this overestimation/underestimation can become significant when increasing the number of devices in the array or decreasing the distances between the devices. Finally, destructive interference is caused by the radiated waves between the devices. This suggests that the optimal layout found by algorithms that ignore the coupling terms might not be accurate because the optimizer should design layouts that create constructive interference. For future work, optimal control of variable-shape wave energy converter arrays will be studied.

Acknowledgement

This material is supported by the National Science Foundation (NSF), USA, under grant number 2023436.

References

[1] J. A. Burton, "Wave catcher," Feb. 9 2012, uS Patent App. 12/851,560.

[2] Y. Sun, A. A. Hamada, O. Sallam, B. Windén, and M. Fürth, "The application of laminar numerical wave tank for a heaving buoy hydrodynamics study in low-turbulence nonlinear waves," *Proceedings of the Institution of Mechanical Engineers, Part M: Journal of Engineering for the Maritime Environment*, p. 14750902231168674, 2023.

[3] A. A. Hamada and M. Furth, "Numerical simulation of the effect of buoy geometries on PTO of wave energy converters," in *Day 3 Fri, October 29, 2021*. SNAME, oct 2021.

[4] M. A. Shabara, S. Zou, and O. Abdelkhalik, "Numerical investigation of a variable-shape buoy wave energy converter," in *International Conference on Offshore Mechanics and Arctic Engineering*, vol. 85192. American Society of Mechanical Engineers, 2021, p. V009T09A013.

[5] A. A. Hamada, A. Rolen, W. McCullough, and M. Furth, "Numerical simulation of the effect of wave characteristics on PTO of point absorber wave energy converter," in *Day 1 Tue, February 22, 2022*. SNAME, feb 2022.

[6] H. Abdulkadir and O. Abdelkhalik, "Optimization of heterogeneous arrays of wave energy converters," *Ocean Engineering*, vol. 272, p. 113818, 2023.

[7] K. Budal, "Theory for absorption of wave power by a system of interacting bodies," *Journal of ship research*, vol. 21, no. 04, pp. 248–254, 1977.

[8] J. Falnes and J. Lovseth, "Ocean wave energy," *Energy Policy*, vol. 19, no. 8, pp. 768–775, 1991.

[9] M. A. Shabara and O. Abdelkhalik, "Optimal control of variable-shape wave energy converters," *IEEE Control Systems Letters*, vol. 7, pp. 1333–1338, 2023.

[10] E. Abraham, "Optimal control and robust estimation for ocean wave energy converters," Ph.D. dissertation, Imperial College London, 2013.

[11] S. Zou, O. Abdelkhalik, R. Robinett, G. Bacelli, and D. Wilson, "Optimal control of wave energy converters," *Renewable energy*, vol. 103, pp. 217–225, 2017.

[12] G. Li, G. Weiss, M. Mueller, S. Townley, and M. R. Belmont, "Wave energy converter control by wave prediction and dynamic programming," *Renewable Energy*, vol. 48, pp. 392–403, 2012.

[13] E. Abraham and E. C. Kerrigan, "Optimal active control and optimization of a wave energy converter," *IEEE Transactions on Sustainable Energy*, vol. 4, no. 2, pp. 324–332, 2012.

[14] D. J. Bell and D. H. Jacobson, *Singular optimal control problems*. Elsevier, 1975.

[15] M. A. Shabara and O. Abdelkhalik, "Dynamic modeling of the motions of variable-shape wave energy converters," *Renewable and Sustainable Energy Reviews*, vol. 173, p. 113070, 2023.

[16] T. Perez and T. I. Fossen, "A matlab toolbox for parametric identification of radiation-force models of ships and offshore structures," 2009.

[17] H. Abdulkadir and O. Abdelkhalik, "Optimal constrained control of wave energy converter arrays," in *2022 American Control Conference (ACC)*. IEEE, 2022, pp. 3100–3105.

[18] Abdulkadir, Habeebullah and Abdelkhalik, Ossama, "Power Constrained Optimal Control of Wave Energy Converters," *IFAC-PapersOnLine*, vol. 55, no. 31, pp. 421–426, 2022.

[19] H. Abdulkadir and O. Abdelkhalik, "Optimal constrained control of arrays of wave energy converters," *Available at SSRN 4274235*.

[20] Habeebullah Abdulkadir and Ossama Abdelkhalik, "Optimization of heterogeneous arrays of wave energy converters," *Ocean Engineering*, vol. 272, p. 113818, 2023. [Online]. Available: https://www.sciencedirect.com/science/article/pii/S0029801823002020

[21] G. Bacelli, *Optimal control of wave energy converters*. National University of Ireland, Maynooth (Ireland), 2014.